DEVELOPMENT OF AN ALGORITHM FOR FAST DNS SIMULATIONS OF CAVITATING FLOWS USING HOMOGENEOUS MIXTURE APPROACH

Anton ŽNIDARČIČ*

Laboratoire de Méchanique de Lille, France

Olivier COUTIER-DELGOSHA

Laboratoire de Méchanique de Lille, France

ABSTRACT

A new algorithm for DNS simulations of cavitating flows is being developed using a form of Kim and Moin projection method. Cavitation is modeled with homogeneous mixture approach and cavitation models' source term can be based either on bubble dynamics or empirical equations. Fast parallel computations are obtained using influence matrix and matrix diagonalization technique.

KEYWORDS

Cavitation, homogeneous mixture approach, turbulence, DNS simulations, mixed boundary conditions

1. INTRODUCTION

Cavitation as a phenomenon is still not completely understood. One of the areas raising many questions is the area of cavitation-turbulence interactions. These are widely studied, mainly experimentally, with numerical work following and adding to experimental results [1], [2].

As numerical simulations offer not just additional, but sometimes also better insight into the flow, they seem to be an interesting tool for obtaining more detailed description of mentioned interactions. There has been a lot of development in the field of numerical simulations of cavitation, from the first models that were able to describe simple, stable cavitation, to the models that are now able to describe not just unstable effects [1], [2], but also include some compressibility effects as in [3]. The most often used models nowadays use homogeneous mixture approach where the density and viscosity of the fluid depend on the volume fractions of present phases which are treated as incompressible. Such models often introduce additional transport equation for vapor volume fraction. Although widely used, they are still not generally applicable to all flow conditions neither give same results if used in identical conditions. Moreover, RANS turbulence models usually accompany them, which leads to error increase, as the models, built on many simplifications, interact with each other.

Consequently, additional attention has to be given to the turbulence-cavitations interactions in numerical simulations in order to obtain better knowledge and better models. A plausible strategy is to perform DNS simulations of cavitating flows and compare the results with experimental data. There were some DNS simulations already performed, but their objective was not the mentioned issue [1], [2], [3]. Moreover, used algorithms could only accept certain

* *Corresponding author:* Laboratoire de Méchanique de Lille, Boulevard Paul Langevin, 59655 Villeneuve d'Ascq, France, phone: +00330320622210 (office 2260), email: anton.znidarcic@ensam.eu

models [1], [2]. Therefore a new algorithm and a code are desired and under development in our laboratory. With them, we intend to perform simulations with mentioned most often used cavitation models that feature additional vapor volume fraction transport equation. As many simulations are to be done, it is requested that the code performs fast DNS simulations.

The aim of this paper is to present the new algorithm and the code. For this reason, the paper is composed as follows: at first, the MFLOPS-3D code, representing a basis for our work, is described. Then, the algorithm is presented through the equations solved in it and the procedure in which it runs. At the end, some verification results are given.

2. MFLOPS-3D code

As fast DNS simulations are needed, it was decided that the in-house code of our laboratory, named MFLOPS-3D, is used as a basis. The code was specially created for fast DNS and LES simulations of incompressible flows. More information about it can be found in [4]. Here, only brief description of its features, important for later parts of the paper, is given.

The code solves the system of governing equations represented by the non dimensional Navier-Stokes momentum and continuity equations, Eq.(1) and (2). The solution algorithm is built on pressure non incremental form of Kim and Moin projection method [5]. This means that firstly, Eq.(1) is put into Helmholtz equation, Eq.(3), to obtain predictor velocity $\vec{u}^*$. The real velocity $\vec{u}$ is found through the projection equation, Eq.(4), which follows from the difference between Eq.(1) and (3). This means that prior to $\vec{u}$, variable Φ has to be obtained, which is done by applying divergence to Eq.(4), thus creating Poisson equation. The boundary conditions for $\vec{u}^*$ and Φ are given in Eq.(5) and (6).

$$\frac{\partial \vec{u}}{\partial t} + \vec{u} \cdot \nabla \vec{u} = -\nabla p + \frac{1}{\mathrm{Re}} \Delta \vec{u} \tag{1}$$

$$\nabla \cdot \vec{u} = 0 \tag{2}$$

$$\left(\Delta - \frac{3\mathrm{Re}}{2dt} \right) \vec{u}^* = \frac{-4\vec{u}^n + \vec{u}^{n-1}}{2dt} + \left(\vec{u} \cdot \nabla \vec{u} \right)^{n,n-1} \tag{3}$$

$$\nabla \Phi = -\frac{3}{2dt} \left(\vec{u} - \vec{u}^* \right) \tag{4}$$

$$\vec{u} \cdot \vec{n} = \vec{u}^* \cdot \vec{n} \qquad ; \qquad \vec{u}^* \cdot \vec{\tau} = \left(\vec{u} + \frac{2dt}{3} \nabla \Phi^n \right) \cdot \vec{\tau} \tag{5}$$

$$\nabla \Phi \cdot \vec{n} = 0 \tag{6}$$

If written, the superscripts in the presented equations define the time level of a certain explicitly treated variable, with *n* being previous time level. In Eq.(5) and (6), $\vec{n}$ and $\vec{\tau}$ depict normal and tangential direction.

Eq.(3) and Poisson equation for Φ form system of equations the code solves in parallel. In each sub domain, a system is solved using matrix diagonalization technique [6]. Diagonalization is done only at the start of a simulation as the left hand side of equations is constant. This is needed because the multidomain method is based on influence matrix technique. Consequently, the most time consuming operations are done only once, at the start, resulting in a code capable of fast DNS simulations.

The code uses structured and collocated grids. Spatial discretization is done with compact finite differences (2^{nd}, 4^{th}, 6^{th} and 8^{th} order can be used), while the time derivative terms use 2^{nd} order backward derivative scheme. The nonlinear term in Eq.(1) is defined with the skew-symmetric form [7], where the 2^{nd} order Adams-Bashford scheme is used for explicit time extrapolation of velocities. This scheme is denoted by *n,n-1* superscript.

3. DEVELOPEMENT AND IMPLEMENTATION OF NEW ALGORITHM

3.1 Governing equations

The governing equations used for the chosen homogeneous mixture approach are the dimensional compressible Navier-Stokes momentum and continuity equations, Eq.(7) and (8). An additional transport equation for vapor volume fraction α, Eq.(9), is added.

$$\rho\left(\frac{\partial \vec{u}}{\partial t}+\vec{u}\cdot\nabla\vec{u}\right)=-\nabla p+\nabla\cdot\left(\mu(\nabla\vec{u})+\mu(\nabla\vec{u})^{T}\right)-\frac{2}{3}\nabla(\mu\nabla\cdot\vec{u}) \tag{7}$$

$$\frac{\partial \rho}{\partial t}+\nabla\cdot(\rho\vec{u})=0 \tag{8}$$

$$\frac{\partial \alpha}{\partial t}+\nabla\cdot(\alpha\vec{u})=\frac{S}{\rho_v} \tag{9}$$

Term S in Eq.(9) is the source term, describing destruction or creation of vapor. Generally, it is a function of pressure p and α. Because the flow in homogeneous approach is treated as one phase flow, represented by a mixture of liquid and vaporous phase, the relationship between the density ρ and viscosity μ of the mixture and both phases is given in Eq.(10). Subscripts v and l stand for vapor and liquid phase.

$$\rho=\rho_v\alpha+(1-\alpha)\rho_l \qquad ; \qquad \mu=\mu_v\alpha+(1-\alpha)\mu_l \tag{10}$$

3.2 The systems of equations composing new algorithm

The new algorithm runs in a similar manner as the one in the original code. But as new governing equations and variables were implemented, the projection method was adapted. The aim of this part of the paper is to present this.

It was found that either pressure incremental or non incremental form of adapted Kim and Moin projection method can be used. This has an important effect on the equation for $\vec{u}^{*}$, Eq.(11). In it, the pressure term is only presented if the pressure incremental form is used.

$$\begin{aligned}\left(\Delta-\frac{3\rho_l}{2dt\mu_l}\right)\vec{u}^{*}=\rho\frac{-4\vec{u}^{n}+\vec{u}^{n-1}}{2dt\mu}+\frac{\rho}{\mu}\left((\vec{u}\cdot\nabla)\vec{u}\right)^{n,n-1}-\frac{1}{\mu}(\nabla\mu)\cdot(\nabla\vec{u}^{n})-\frac{1}{\mu}(\nabla\mu)\cdot(\nabla\vec{u}^{n})^{T}\\ -\frac{1}{3}\nabla(\nabla\cdot\vec{u}^{n})+\frac{2}{3\mu}\nabla\mu(\nabla\cdot\vec{u}^{n})+\frac{\nabla p^{n}}{\mu}+\left(\frac{3\rho}{2dt\mu}-\frac{3\rho_l}{2dt\mu_l}\right)\vec{u}_{e}^{\,*}\end{aligned} \tag{11}$$

Eq.(11) is derived from Eq.(7) in same manner as in the original Kim and Moin method. The obvious difference is increased number of explicitly treated terms, resulting from the viscous stress term. ρ and μ are also treated explicitly, like velocity $\vec{u}$. In order to decrease the amount of explicitly treated terms and preserve constant left hand side, the Concus and Golub (C&G from here on) method is used [8]. This gives the last term in Eq.(11) and demands performing iterative steps until $\vec{u}^{*}$ and its explicit approximation $\vec{u}_{e}^{\,*}$ converge (convergence criteria is set to 10^{-4} absolute difference between iterations).

After $\vec{u}^{*}$ is obtained, the projection equation has to be solved. The variable Φ is used in it as it was found impossible to solve directly for pressure p. The projection equation follows from the difference of equations Eq.(7) and (11) and can be written in two forms, depending on the fact if density is excluded from Φ (Eq.(12)) or not (Eq.(13)).

$$\nabla\Phi = -\frac{3\rho}{2dt}\left(\vec{u} - \vec{u}^{*}\right) \tag{12}$$

$$\nabla\Phi = -\frac{3}{2dt}\left(\vec{u} - \vec{u}^{*}\right) \tag{13}$$

In order to solve for Φ, divergence is applied to Eq.(12) or (13). Important here is the replacement of the unknown divergence of $\vec{u}$ with source term S using the connection in Eq.(14). This results in Poisson equations for Φ, Eq.(15) and (16), obtained from Eq.(12) and (13), respectively, and makes their solution possible [9].

$$\nabla \cdot \vec{u} = S\left(\frac{1}{\rho_v} - \frac{1}{\rho_l}\right) \tag{14}$$

$$\Delta\Phi = -\frac{3\left(\vec{u} - \vec{u}^{*}\right)}{2dt} \cdot \nabla\rho - \frac{3\rho}{2dt}\left(S\left(\frac{1}{\rho_v} - \frac{1}{\rho_l}\right) - \nabla \cdot \vec{u}^{*}\right) \tag{15}$$

$$\Delta\Phi = -\frac{3}{2dt}\left(S\left(\frac{1}{\rho_v} - \frac{1}{\rho_l}\right) - \nabla \cdot \vec{u}^{*}\right) \tag{16}$$

It should be noted however, that Eq.(15) and (16) are written as if current $\vec{u}$ or S are known, the actual solution procedure for Φ is given later. With known Φ, one can easily obtain values of $\vec{u}$ by using Eq.(12) or (13). Pressure needs to be determined as well. Connections of p with Φ and $\vec{u}$ depend on the use of pressure non incremental or incremental form and equations for Φ. If non incremental form is used, the connection was, similary as in [5], proved to be given with Eq.(17) (in case of using Eq.(12)) or with Eq.(18) (when Eq.(13) is used).

$$p = \Phi + \mu\left(S\left(\frac{1}{\rho_v} - \frac{1}{\rho_l}\right) - \nabla \cdot \vec{u}^{*}\right) \tag{17}$$

$$p = \rho\Phi + \mu\left(S\left(\frac{1}{\rho_v} - \frac{1}{\rho_l}\right) - \nabla \cdot \vec{u}^{*}\right) \tag{18}$$

The Φ-p connection in case of pressure incremental form is obtained from Eq.(17) and (18) by adding the pressure from previous time step and neglecting the viscous terms, as $\vec{u}$ and $\vec{u}^{*}$ are nearly the same [10]. Once p is known, source S can be updated with it.

The last equation that needs to be solved is transport equation for α. This equation cannot be reshaped into a Helmholtz equation and solved with the solver. As the most important variables are known, we solve it for each point separately as given in Eq.(19).

$$\alpha^{n+1,k+1} = \frac{\frac{S^{n+1,k}}{\rho_v} + \frac{4\alpha^{n} - \alpha^{n-1}}{2dt} - \left(\vec{u}^{\,n+1} \cdot \nabla\right)\alpha^{n+1,k}}{\frac{1}{2dt} + S^{n+1,k}\left(\frac{1}{\rho_v} - \frac{1}{\rho_l}\right)} \tag{19}$$

The solution follows iterative procedure, where k denotes the iteration step. Source S is updated also. After α is obtained (considered converged when 10^{-8} absolute difference is reached), density and viscosity are updated using Eq.(10) before going to the next time step.

3.3 Boundary conditions

Special attention has to be given to boundary conditions. When $\vec{u}^*$ is considered, conditions follow the same logic as in the original code. Example is given in Eq.(20) for the case of using Eq.(12). However, the conditions for the Poisson equation were changed. The reason is that for Φ to be successfully solved, von Neumann conditions demand fulfillment of compatibility condition [11]. This effectively means that the mass flow in the domain has to be known in advance or constant, which does not apply to our problem. Therefore mixed boundary conditions were introduced for Φ. Dirichlet conditions were imposed on the exit of the domain in form of pressure and not Φ values. Using the latter proved to actually result in unstable simulations. Homogeneous von Neumann conditions were used elsewhere. This relaxed the compatibility condition and greatly improved stability and speed of simulations.

$$\vec{u}\cdot\vec{n}=\vec{u}^*\cdot\vec{n} \quad ; \quad \vec{u}^*\cdot\vec{\tau}=\left(\vec{u}+\frac{2dt}{3\rho}\nabla\Phi^n\right)\cdot\vec{\tau} \tag{20}$$

Boundary conditions for α in form of Dirichlet conditions had to be imposed as well.

3.4 Solution procedure for Φ

Solution for Φ proved to be the most difficult. The main issue is that the divergence of $\vec{u}$ or the term S are not known in advance. Moreover, using explicit S results in low stability [9]. Known remedy is to linearize S, usually in regards to pressure, and use the resulting derivative term on the left hand side of the system of equations [9]. In our code, such an operation cannot be copied because of the demand for constant left hand side of equations and because we solve for Φ and not p. Therefore another procedure was developed. After trying different settings, it was found that the best results are obtained if S is fully linearized, as given in Eq.(21). The $d\alpha$ term in it was then reshaped using Eq.(9) and material derivative definition into form in Eq.(22), which includes term dp. Therefore linearized source term includes two terms with dp, which are then connected to Φ by the use of corresponding equations for p-Φ connection. With this, we introduce Φ on this side of equation. If Poisson equation form for Φ is retained, the Φ on the right hand side has to be explicitly treated. Iterations are performed until Φ converges, but as observed in [9], procedure offers low stability. However, using C&G method by introducing a constant factor σ (where σ value originates from the terms including Φ), as example in Eq.(23) depicts, proved to give stable and also faster simulations. This procedure is therefore used as the solution procedure for Φ.

$$S^{n+1}=S^n+\frac{\partial S}{\partial p}dp+\frac{\partial S}{\partial \alpha}d\alpha \tag{21}$$

$$d\alpha=\frac{S^n+\dfrac{\partial S}{\partial p}dp}{\dfrac{1}{K}-\dfrac{\partial S}{\partial \alpha}} \quad ; \quad K=\left(\frac{1}{\rho_v}-\alpha^n\left(\frac{1}{\rho_v}-\frac{1}{\rho_l}\right)\right)dt \tag{22}$$

$$(\Delta+\sigma)\Phi^{k+1}=-\frac{3}{2dt}\left(\left(S^n+\frac{\partial S}{\partial p}dp+\frac{\partial S}{\partial \alpha}d\alpha\right)\left(\frac{1}{\rho_v}-\frac{1}{\rho_l}\right)-\nabla\cdot\vec{u}^*\right)+\sigma\Phi^k \tag{23}$$

In Eq.(21)-(23), α and S are explicit and only Φ is updated during iterations. When it converges (convergence criteria is set to 10^{-3} absolute difference between two iterations), the velocity is updated using corresponding projection equation. Same applies to pressure and

source term. If Φ is solved using Eq.(15), the velocity $\bar{u}$ is also updated during iterations using Eq.(12).

3.5 Other implemented numerical methods

Additional numerical methods were also implemented in the code to improve stability and performance. Upwind derivatives of first and second order were implemented to describe the α advection term in Eq.(19), as the use of compact finite differences resulted in oscillations. Because of this and to ensure derivatives consistency, the corresponding upwind schemes were also used for the density and viscosity derivatives. Explicit source term S^n replaced the explicit velocity divergence term in Eq.(11) following the same reasons. Finally, the use of compressible Navier-Stokes equations demanded the change of original non linear term skew-symmetric form with the skew-symmetric form for compressible cases, obtained from [12].

4. NUMERICAL EXPERIMENTS-VERIFICATION OF THE ALGORITHM

The algorithm was up to now mainly tested with a verification process based on the use of Method of Manufactured Solutions [13]. Analytical flow equations describing the flow with variable density and corresponding source term S have been developed and used to see if the algorithm solves the system of governing equations in a correct manner. Example of such equations, used also in the tests presented below, is given in Eq.(24)-(27).

$$u = C\cos(gt)\cos(ay) \tag{24}$$

$$v = \left(1-\frac{\rho_v}{\rho_l}\right)\frac{\left(BC\cos(gt)\sin(gt)\cos(ax)\sin(ay)+Bg\cos(gt)\sin(ax)y\right)}{1-\left(1-\frac{\rho_v}{\rho_l}\right)\left(K_1+B(\sin(gt)\sin(ax)+1)\right)} \tag{25}$$

$$p = \frac{\left(BCa\cos(gt)\sin(gt)\cos(ax)\cos(ay)+Bg\cos(gt)\sin(ax)\right)}{\left(K_1+B(\sin(gt)\sin(ax)+1)\right)\left(\left(1-\frac{\rho_v}{\rho_l}\right)\left(K_1+B(\sin(gt)\sin(ax)+1)\right)-1\right)} \tag{26}$$

$$\alpha = B(\sin(ax)\sin(gt)+1)+K_1 \qquad ; \qquad S = -\alpha p\rho_v \tag{27}$$

The velocity w in z direction is 0 *m/s*, the constant K_1 describes minimum α. The values g and a are used to govern time and spatial frequency, respectively, while C and B define the amplitude of velocity and α fluctuations. Examples of solutions, obtained with the new algorithm for pressure incremental and non incremental forms with the use of Eq.(15) for Φ, are given in Fig.1. The factors σ, used for the C&G method in incremental and non incremental forms, are given in Eq.(28) and (29), respectively. They follow the recommendation in [8] to be chosen as the middle value of possible values (the subscript denotes that values are given for α=0,5). The domain size in the shown case is {-0,2;0,2} *m* in x and y direction, {-0,1;0,1} *m* in z. Domain is composed of four sub domains, each containing 21 points in x,y directions and 11 points in z, forming non-uniform mesh. The time step is dt=0,014 *s*, 1800 time steps were done, with $C=1$, $B=0,5$, $a=2\pi$ and $g=\pi$. Phases are chosen to have ρ_l=10 *kg/m*^{3}, ρ_v=3 *kg/m*^{3}, μ_l=0,05 *Pa·s* and μ_v=0,01 *Pa·s*.

$$\sigma = -\frac{3}{2dt}\alpha_{0,5}\rho_{0,5}\left(1-\frac{\rho_v}{\rho_l}\right) \tag{28}$$

$$\sigma = -\frac{3}{2dt}\frac{\alpha_{0,5}\rho_{0,5}}{1+\mu_{0,5}\rho_v\alpha_{0,5}\left(\frac{1}{\rho_v}-\frac{1}{\rho_l}\right)}\left(1-\frac{\rho_v}{\rho_l}\right) \tag{29}$$

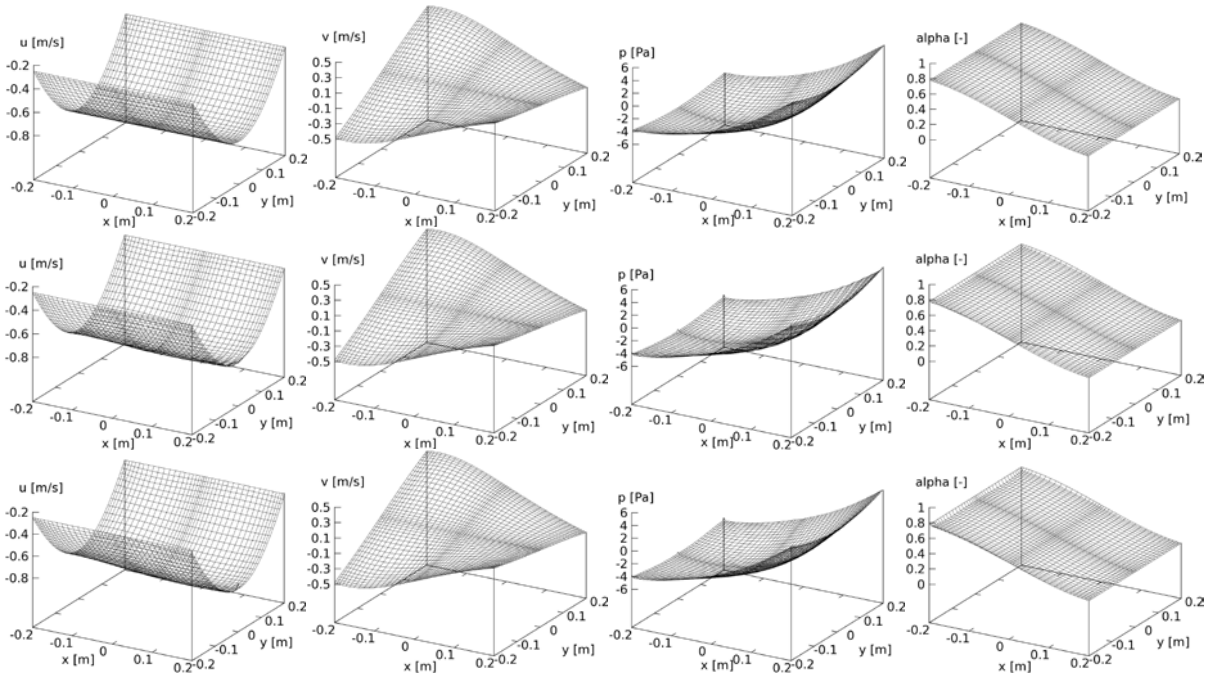

Fig.1 Example of analytical values and obtained results for a test case using MMS.

On Fig.1, plots of *u*, *v* velocity, pressure *p* and α at *z*=0 *m* are shown from left to right. Top line presents analytical values, following equations Eq.(24)-(27). Solutions obtained with pressure incremental form are given in the middle and solutions for non incremental form on the bottom. It can be seen that results with both forms are correct, with small deviations from analytical values. The pressure incremental form proved to be faster for cca 10% than non incremental, due to a bit less iterations for $\vec{u}^*$ and Φ. In both forms, typically 4 to 7 iterations are done for *u*, 3 to 5 for *v* and 2 to 3 for *w* ($\vec{u}^*$ components), while Φ takes from 3 to 8 iterations to converge, depending on current α range.

The biggest error to be noted is in α solution, near the boundaries. While this causes no issues if Eq.(15) is used, it results in oscillations of pressure and lower stability when using Eq.(16). The reason is that the pressure with it is obtained through $\Phi\rho$ multiplication, introducing α solution error directly into *p*. Using Eq.(16) is nevertheless retained in the code, as it might not suffer from this effect in real flow simulations (α=0 at the boundary, possibly removing the error). And following [9], using it can give improvement of possible α dispersion error.

To assess how well the algorithm actually performs, tests with pure Dirichlet boundary conditions for Φ (*p* values are taken from Eq.(26)) were performed also. These give ideal performance of the algorithm regarding stability and speed. It was found that the algorithm with such boundary conditions performs to 30 % faster, while the stability is practically no better. The case presented on Fig.1 actually presents nearly the limiting case (regarding the values of *B*, *C*, *a* and *g*) that our new algorithm and also the algorithm using Dirichlet conditions can stably solve. For example, they both diverge once constant *C* exceeds value of 1,25. Therefore we can conclude that the presented algorithm and the code are ready to be used in more demanding, real flow simulations. This was not done up to now because of the computational intensity and time demands of such simulations.

5. CONCLUSION

The paper presents a new algorithm suitable for fast DNS simulations of cavitating flows with homogeneous mixture approach. The algorithm is based on the adapted Kim and Moin projection method and offers multiple ways in which the governing equations can be solved. The most stable are those using Eq.(12) for Φ. The algorithm shows practically same performance stability wise when compared to the ideal conditions in which equations can be solved and is therefore considered to be suitable for performing real flow DNS simulations of cavitation. Besides cavitating flows, the algorithm could also be used for simulations of other multiphase flows, where homogeneous mixture approach is used and present phases are considered incompressible.

6. ACKNOWLEDGEMENT

The work is funded by the DGA-Direction générale de l'armement - French government defense procurement agency.

7. REFERENCES

[1] Kubota, A.,Kato, H., Yamaguchi, H.: *A new modelling of cavitating flows: a numerical study of unsteady cavitation on a hydrofoil section.* J. Fluid Mech. Vol. 240. pp.59-96.

[2] Xing, T., Li, Z., Frankel, S.: *Numerical Simulation of Vortex Cavitation in a Three Dimensional Submerged Transitional Jet*. J. Fluids Engrg. Vol. 127. pp. 714-725

[3] Lu, T., Samulyak, R., Glimm, J.: *Direct Numerical Simulation of Bubbly Flows and Application to Cavitation Mitigation*. J. Fluids Engin. Vol. 129. pp. 595-604

[4] Marquillie, M., Laval, J.P., Dolganov, R.: *Direct numerical simulation of a separated channel flow with a smooth profile. Journal of Turbulence,* Vol. 9. pp. 1-23

[5] Guermond, J.L., Minev, P., Shen, J.: *An overview of projection methods for incompressible flows*. Comput. Methods Appl. Mech. Engrg. Vol. 195. pp. 6011-6045

[6] Haldenwang, P. et al.: *Chebyshev 3-d spectral and 2-d pseudospectral solvers for the helmholtz equation*. Journal of Comp. Physics. Vol. 55. pp. 115-128

[7] Morinishi, Y. et al.: *Fully conservative higher order finite difference schemes for incompressible flow*. Journal of Comp. Physics. Vol. 143. pp. 90-124

[8] Dimitropoulos, C.D., Beris, A.N.: *An efficient and robust spectral solver for nonseparable elliptic equations*. Journal of Comp. Physics, Vol. 133. pp. 186-191

[9] Sauer, J.: *Instationar kavitierende Stromungen-Ein neues Modell*. PhD thesis, Fakultat fur Mashinenbau der Universitat Karlsruhe. 2007.

[10] Brown, D.L.: *Accurate Projection Methods for the Incompressible Navier–Stokes Equations*. Journal of Comp. Physics, Vol. 168. pp. 464-499

[11] Abide, S., Viazzo, S.: *A 2D compact fourth-order projection decomposition method.* Journal of Comp. Physics, Vol. 206. pp. 252-276

[12] Morinishi, Y.: Skew-symmetric form of convective terms and fully conservative finite difference schemes for variable density low-Mach number flows, Journal of Comp. Physics, Vol. 229. pp. 276-300

[13] Eca, L., Hoekstra, M.: *Code verification of unsteady flow solvers with the method of manufactured solutions. Proceedings of the Seventeenth International Offshore and Polar Engineering Conference*, ISOPE, 2007